PROTEINS: Structure, Function, and Bioinformatics 67:931–940 (2007)

The Structural Properties of Magainin in Water, TFE/Water, and Aqueous Urea Solutions: Molecular Dynamics Simulations

Faramarz Mehrnejad, Hossein Naderi-Manesh,* and Bijan Ranjbar
Faculty of Science, Department of Biophysics, Tarbiat Modarres University, Tehran, Iran

ABSTRACT **Here, the MD simulations and comparative structural analysis of Magainin in water, TFE/water, and 2M, 4M, and BM urea solutions is reported. For MAG-TFE/water and MAG-2M urea the largely alpha helical conformation of the peptide is maintained throughout the 9-ns simulation. While in water, 4M urea, and 8M urea, the helix length decreases and at the same time helix radius increases. This suggests a more destabilized magainin secondary structure. Our simulation data reveals that the stabilizing effect of TFE is induced by preferential accumulation of TFE molecules around the alpha helical peptide. These results indicate that an aqueous urea solution solvates the sutface of polypeptide chain more favorably than pure water. Urea molecules interact more favorably with nonpolar groups of the peptide in comparison with water, and the presence of urea improves the interactions of water molecules with the hydrophilic groups of the peptide. At 8M urea, there are more direct interactions between the urea and solute, and the helix is destabilized. At 2M urea, the interaction of urea molecules and nonpolar residues are weak, therefore, the presence of urea molecules decreases the interactions of water molecules with hydrophilic groups. Urea could not deteriorate the peptide secondary structure with time from an initial helix structure. Proteins 2007;67:931–940.** © 2007 Wiley-Liss, Inc.

Key words: Molecular Dynamics Simulations; GROMACS; Secondary Structure; Alpha Helix; Aqueous Urea Solution

INTRODUCTION

Protein and peptide stability is the result of a balance between the intramolecular interactions of protein functional groups and their interactions with the solvent environment. Addition of cosolvents into the protein solution can modify this balance.[1,2] Presence of small organic molecules in aqueous solution can also have profound effects on protein stability, structure, and function. The use of these solutions to stabilize or destabilize proteins, depending on the cosolvent, is common. In fact, protein studies are conducted almost exclusively in complex solutions. The addition of cosolvents to solutions of peptides and proteins can result in a variety of effects such as denaturation, increased or decreased solubility, and secondary structure formation.[3,4] The natural solvent for protein is water, but it is always mixed with cosolvents, which influences the ionic strength, the pH values, and the chemical affinity to certain molecular groups on the protein surface, and so forth. These properties naturally have a tremendous influence on protein stability; they can induce unfolding or refolding, and may as well lead to significant changes of the critical physical parameters, that is, the critical temperature and the critical pressure, which determine the phase boundaries between the native and denatured states. The physical properties of water, such as its ability to form hydrogen bonds, the hydrophobic and hydrophilic interaction with respective amino acids, the high specific heat of locally ordered structures, structure and density variations, and so forth, have a strong influence on the stability boundaries.[5]

Cosolvent

Chemical denaturation, with an agent such as urea, is one of the primary ways to assess protein stability, the effects of mutations on stability, and protein unfolding.[6] Although urea is widely used as denaturant agents, it is still not clear by which molecular mechanism urea denatures proteins. It is well known that the solubility of the most protein side chains and backbone increases with denaturate concentration.[7] Urea is very soluble in water, and its high concentration is often required to observe denaturation[8] while, there is still some uncertainty about the dominant manner by which it acts.[9–12] There are two main models for urea-induced denaturation.[11] In the first model, urea interacts directly with the protein, particularly by hydrogen bonding to polar groups competing with intramolecular hydrogen bonding. In the other model, the effects are indirect, that is, urea changes the hydrogen bonding network of the solvent around hydrophobic groups, providing a better solvation environment

*Correspondence to: Hossein Naderi-Manesh, Faculty of Science, Department of Biophysics, Tarbiat Modarres University, Tehran, Iran. E-mail: naderman@modares.ac.ir

Received 23 June 2006; Revised 27 September 2006; Accepted 6 October 2006

Published online 13 March 2007 in Wiley InterScience (www.interscience.wiley.com). DOI: 10.1002/prot.21293

and reducing the hydrophobic effect. Overall, the previously reported protein MD simulations support the role of both of these effects in urea denaturation.[8,13–15]

2,2,2-Trifluoroethanol (TFE) is another cosolvent that has been used to study peptides in solution specially since experimental studies show that the presence of TFE increases the population of α-helix content in secondary structure forming peptides in TFE/water mixtures.[3,16] Despite many experimental and theoretical studies, the mechanism by which TFE affects the structure and dynamics of peptides and proteins is still unclear.[3] One possible explanation is the preferential solvation of the folded state by TFE. According to this hypothesis, TFE acts within the context of preexisting helix-coil equilibrium, and the preferential interaction of TFE with the folded state shifts the equilibrium toward more structured conformations.[17] The molecular nature of the TFE-peptide interactions is not clear, however, alternative mechanisms have also been proposed to explain the stabilizing effect of TFE. In particular, the effect could result from TFE reinforcing hydrogen bonds between carbonyl and amidic NH groups by the removal of water molecules in the proximity of the solute[18] and/or the lowering of the dielectric constant.[3] Computer simulations indicate a coating effect of TFE on the simulated peptides, as a possible mechanism of peptide stabilization.[19–21]

The Peptide

Magainin 2 is a 23-residue long, amphipathic, α-helical antimicrobial peptide that is secreted by the skin of the African frog *Xenopus laevis*. The sequence of the peptide is as follow: GIGKFLHSAKKFGKAFVGEIMNS. Its structure has been determined by NMR spectroscopy. The NMR structures were determined in detergent micelles and nonpolar solvent.[22] These studies indicate that magainin adopts a very similar α-helical conformation in different environments. Magainin has attracted much attention due to its significant random coil structure in water. Diverse experiments show that the stability of the magainin α-helix depends on solvent environment. Molecular dynamics simulations can provide valuable information about the various stages of peptide-solvent interactions. The effect of solvent and bilayer on the stability of the magainin α-helix has been investigated previously by different authors using molecular simulation methods.[22–25] In simulation studies in TFE/water and in a membrane environment, magainin stayed close to the experimental α-helical structure, whereas in water it starts to bend and unfolds.[22]

The goal of our simulations is to perform a comparative analysis on interaction of TFE (membrane-mimicking cosolvent) and different concentrations of urea with helical antimicrobial peptide only in nano second time scale. The previous studies suggest that magainin form stable helical structures in the membrane environment, while it destabilizes into a random coil in a pure water environment.[25] These properties help us to investigate the molecular level and the structural effects of different concentrations of urea on this α-helical peptide.

METHODS

The GROMACS program with the all-atom parameter set was used in all MD simulations.[26,27] Before starting the dynamics simulations, each system was energy-minimized by using a steepest descent algorithm for 100 steps. In all simulations, the temperature and the pressure were kept close to the intended values (300 K and 1 bar) by using the Berendsen algorithm[28] with $\tau_T = 0.1$ ps and $\tau_p = 0.5$ ps, respectively. The GROMOSE96 force field[29] was used to describe the peptide. Simulations were run with a 2-fs time steps. Bond length was constrained using the LINCS algorithm.[30] Lennard–Jones interactions were calculated with a 0.9/1.4-nm twin-range cut off. The short-range electrostatic interactions were calculated to1.0 nm, and Particle Mesh Ewald algorithm was used for the long-range interactions.[31] The neighbor list was updated every 10 steps. Each component of the systems (i.e., peptide, water, urea, and TFE) was coupled separately to a temperature bath at 300 K, using a Berendsen thermostat[32] with a coupling constant $\tau_T = 0.1$ ps. In the water, urea/water, and 33% trifluoroethanol (TFE)/water simulations, the pressure was kept at 1.0 bar using isotropic pressure coupling[32] with $\tau_p = 0.5$.

The initial structure of peptide was obtained from the PDB databank.[22] The peptide was solvated with either SPC water[33] or a mixture of urea or mixture of TFE and SPC water and placed in a cubic large enough to contain the peptide and 0.8 nm of solvent on all sides. Counter ions (Cl and Na, respectively) were added by replacing water molecules at the most positive/negative electrical potential to achieve a neutral simulation cell.

The concentration (% v/v) TFE and urea molecules around the peptide residues, named local TFE concentration (LTC) and local urea concentration (LUC), was evaluated from the cumulative number of water [$n_w(r)$], TFE [$n_T(r)$], and urea [$n_U(r)$] molecules present within a distance r from the C_αs of the single residues using the following relation:

$$\mathrm{LTC}(r) = \frac{V_m^T n(r)}{[V_m^T n(r) + V_m^W n_W(r)]} \times 100 \qquad (1)$$

where $V_m^T = 0.07$, $V_m^W = 0.019$, and $V_m^U = 0.046$ L/mol are average excluded volumes for TFE, water, and urea molecules.[34]

RESULTS AND DISCUSSION

Root Mean-Square Deviation

In Figure 1, the root mean-square deviation (RMSD) with respect to the initial structure for the peptide in pure water, TFE/water, 2, 4, and 8*M* urea as a function of time is reported. The magainin backbone remained practically unchanged along TFE/water and 2*M* urea simulations, with an RMSD average below 2.5 Å [Fig. 1(A)]. This suggests that the peptide NMR structure is largely maintained its native structure in 2*M* urea and TFE/water, at least on the time scale sampled in these simulations. As found previously,[25] magainin is unstable over-

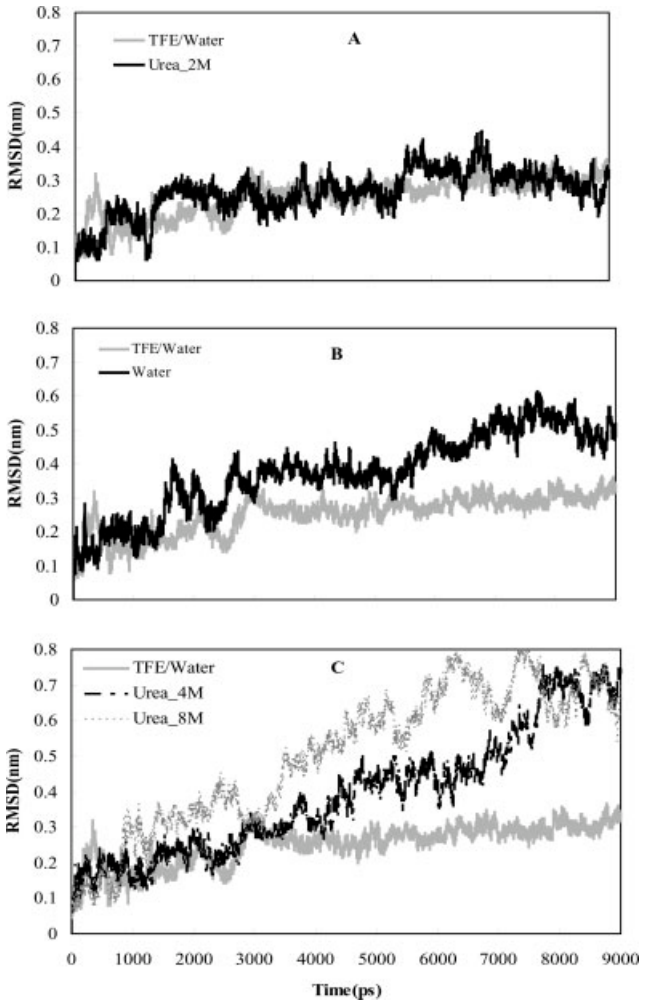

Fig. 1. Atom-positional root mean-square deviation (RMSD) of magainin with respect to the initial NMR structure for the simulations MAG-TFE/water and MAG-2*M* urea (**A**), MAG-TFE/water and MAG-water (**B**), MAG-TFE/water, MAG-4, and MAG-8*M* urea.

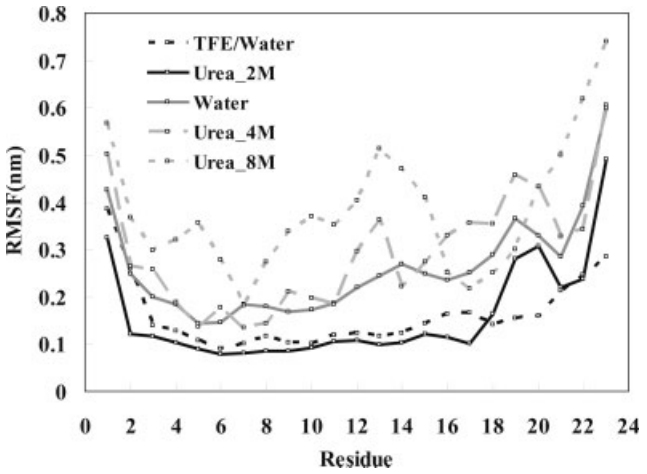

Fig. 2. The backbone atomic positional RMSF of magainin in TFE/water, 2*M* urea, water, 4, and 8*M* urea simulations.

time range of the water run. After 2.5 ns in water, the RMSD reached values up to 3.5 Å [Fig. 1(B)]. In 4*M* urea, the RMSD rises almost continuously over the first ~4.5 ns, to a peak of ~0.4 nm [Fig. 1(C)]. Magainin began to gradually unfold, from the first picoseconds of the 8*M* urea simulation [Fig. 1(C)].The backbone RMSD values were somewhat higher in the 8*M* urea simulation. The instability of peptide in pure water has been observed by using different MD protocols.[25] In contrast to its behavior in pure water, in the TFE/water mixture and 2*M* urea, MAG is stable with the RMSD remaining almost constant at around 0.25 nm for the first 5 ns of the simulation, rising to 0.31 nm during the last 4 ns. In Figure 2, the C-α RMS fluctuations from the average are examined as a function of residue number. These results confirm the similarity of MAG-TFE/water and MAG-2*M* urea simulations and their differences from MAG-water, MAG-4*M*, and 8*M* urea concentrations. The average atomic RMSFs of magainin were 0.15 nm in 2*M* urea, 0.16 nm in TFE/water mixture, 0.26 nm in water, 0.29 nm in 4*M* urea, and 0.38 nm in 8*M* urea. Thus, the RMSF per residue for the overall mobility of residues in water, 4, and 8*M* urea is larger than that of the 2*M* urea and TFE/water mixture (Fig. 2). Thus, for MAG-TFE/water and MAG-2*M* urea, the C-α RMSF versus residue plot is relatively flat. Except for the terminal residues, the fluctuations in 2*M* urea and TFE/water are less than 0.12 nm, and for the central core they are nearly 0.1 nm. The corresponding graph for magainin in water, 4, and 8*M* urea is markedly different. In water, the overall magnitude of the RMSFs is higher, ranging from 0.13 to 0.36 nm. The RMSFs confirm the peptide helix is stable in 2*M* urea and TFE/water environment but less stable in water solution and high concentration of urea, where disordering of the C-terminal half of the molecule occurs.

Secondary Structure

The secondary structure of the peptide during the course of the simulations is shown in Figure 3, as defined by dictionary of secondary structure of proteins (DSSP).[35] In all cases, the peptide secondary structure deteriorates with time from an initial helix structure. Comparison of MAG-2*M* urea and MAG-TFE/water with MAG-water reveals a major difference. For MAG-TFE/water and MAG-2*M* urea, the largely α-helical conformation of the peptide is maintained throughout the 9-ns duration of the simulation. There are occasional local deviations from α-helicity in the C-terminal part of the molecule (Fig. 4). In water, the α-helicity of peptide decreases at the C-terminus of the molecule starting at 1.5 ns and reaching its maximum extent at 3.2 ns (Fig. 3). The N-terminal segment remains α-helical, whereas the C-terminal segment switches dynamically between 5-helix, turn, and bend conformations. After 3.5 ns, residues 1–7 remain in an α-helical conformation, residues 7–20 fluctuate between five-helix and turn conformation (Fig. 3). Helix radius and helix length are a few quantitative measure of the degree of secondary structure deterioration, and Figure 5

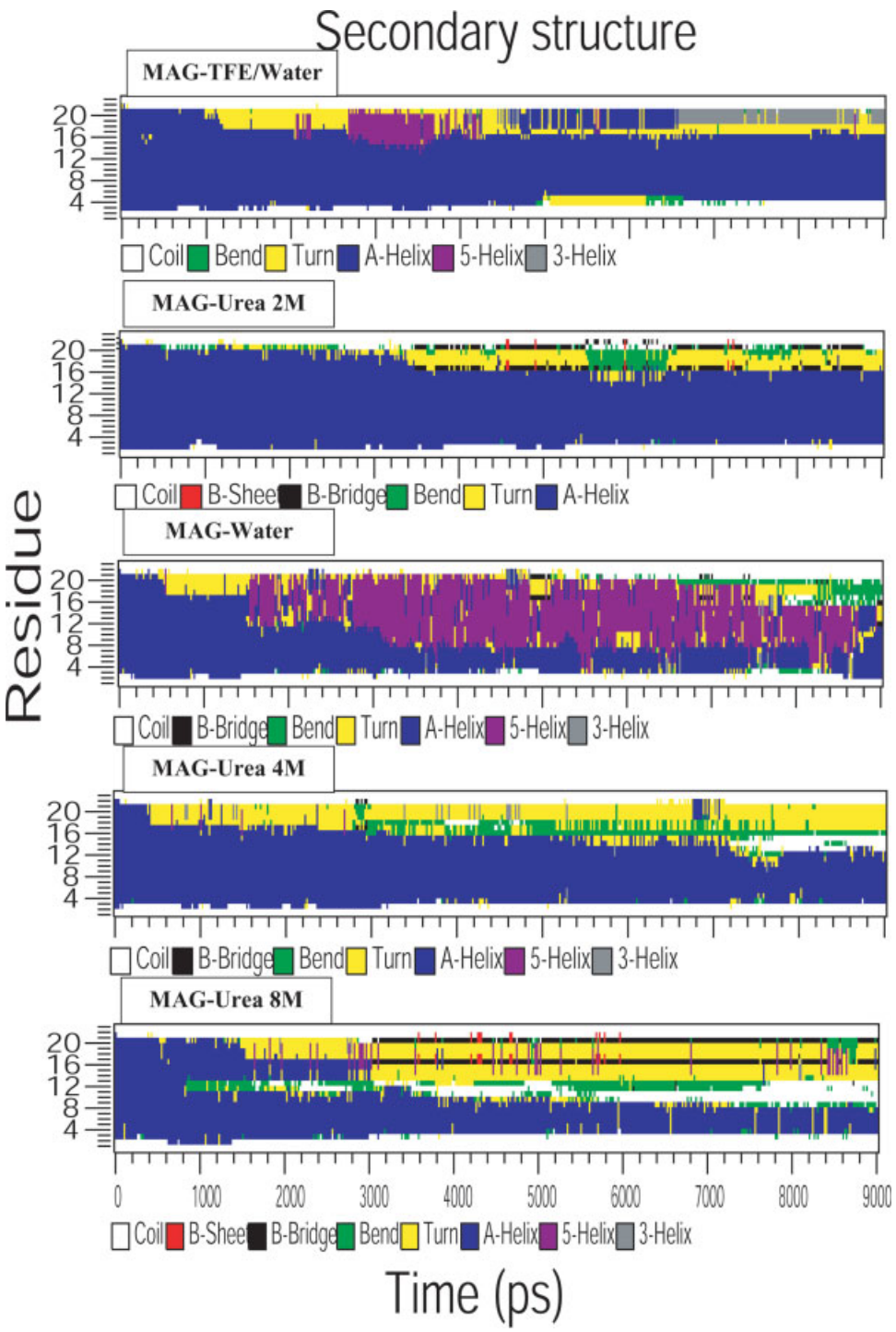

Fig. 3. Secondary structures of the peptide in simulations: MAG-TFE/water, MAG-2*M* urea water, 4, and 8*M* urea.

shows these properties as a function of time. In water, in 4*M* urea, and in 8*M* urea, the helix length decreases while, helix radius increases, thus it moves toward a more destabilized magainin secondary structure. These results clearly show that the peptide becomes destabilized in water, in 4*M* urea, and in 8*M* urea too.

Hydrogen Bond

The analysis of the intramolecular backbone hydrogen bonds basically reflects the observations made in the conformational analysis of the simulations (Table I). Hydrogen bonds characteristic for the α-helical conformation

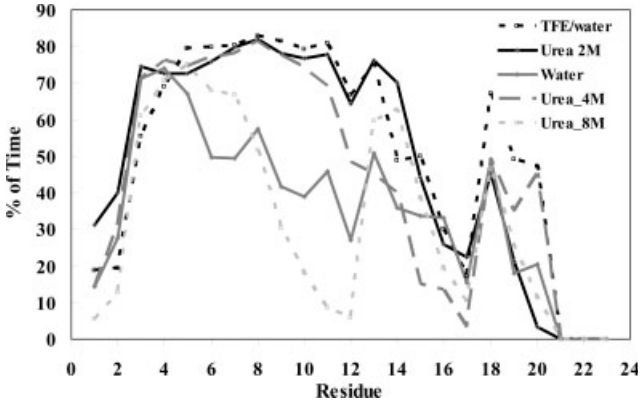

Fig. 4. The helicity per residue of magainin: MAG-TFE/water, MAG-2M urea water, 4, and 8*M* urea simulations.

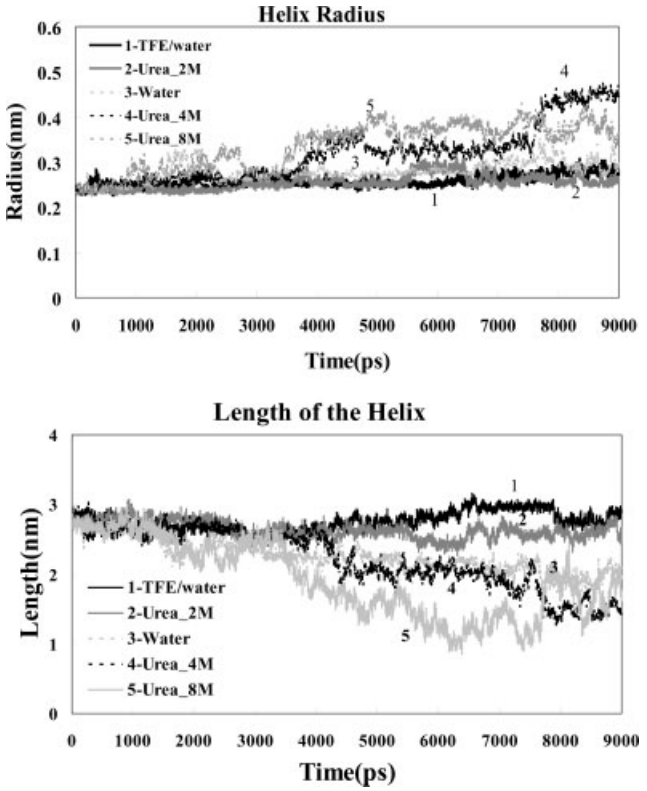

Fig. 5. The helix radius and helix length as a function of time: the helix radius increases and the helix length decreases in all the simulations, showing peptide instability in water, 4, and 8*M* urea simulations.

are largely populated in MAG-TFE/water and MAG-2*M* urea environment, while in water residues, Leu^{6}-Ile^{2}, His^{7}-Gly^{3}, Ser^{8}-Lys^{4}, and Phe^{16}-Lys^{11} show more than 70% hydrogen bond populations. In MAG-4*M* urea, the α-helical hydrogen bonds appear to be less populated in 15–22 region, while in MAG-8*M* urea, the α-helical hydrogen bonds disappear in 11–16 region of the peptide. Sequential loss of the stable hydrogen bonding for residues Ala^{9}-Phe^{5}, Lys^{10}-Leu^{6}, Lys^{11}-His^{7}, Phe^{12}-Ser^{8}, Lys^{14}-Lys^{10}, and Phe^{16}-Phe^{12} occurs throughout the simulation in the water and 8*M* urea environments (Table I). The most C-terminus α-helical hydrogen bond practically disappeared. Unwinding started from C-terminus and propagated toward the N-terminus. In water, the peptide backbone very quickly lost its α-helical hydrogen bonds beginning from its C-terminus and propagating toward the N-terminus. In 8*M* urea, the backbone lost its α-helical hydrogen bonds beginning from its middle of peptide and propagating toward the C-terminus and N-terminus. The α-helical content (i, $i + 4$ hydrogen bonds) were monitored along the trajectory (Fig. 6). The six initial α-helical hydrogen bonds formed by MAG were maintained during the entire simulations in TFE/water and 2*M* urea, while there were not maintained during the simulation of 8*M* urea. In the water simulation, the all α-helical hydrogen bonds disappeared completely after 2.5 ns of simulation. In TFE/water and 2*M* urea, the final structure contained all six intrabackbone hydrogen bonds. In water simulation, the peptide rapidly lost its six initial α-helical hydrogen bonds, converting into π-helical hydrogen bonds in a cooperative manner from the C-terminus toward the N-terminus, and on some occasions coexisting with them. In water as well as in urea, the α-helical hydrogen bonds were lost completely or were turned into π-helical hydrogen bonds. However, in 8*M* urea, disruption of α-helical hydrogen bonds did begin not only at the C-terminus but also at the middle of the helix. Figure 7 shows the total number of hydrogen bonds between the peptide and solvents over the course of the simulations. In MAG-TFE/water, the total number of hydrogen bonds between peptide and TFE increases with time and the total number of hydrogen bonds between peptide and water decreases. The simulation shows that the organic cosolvent accumulates around the peptide forming a matrix that partly excludes water. By accumulating around the solute the TFE molecules exclude water, favoring the formation of intramolecular hydrogen bonds and promoting the formation of secondary structure. In MAG-2*M* urea, the total number of peptide–water, peptide–urea, and intramolecular peptide–peptide hydrogen bonds remain constant with time, while in MAG-4*M* urea, the total number of hydrogen bonds between the peptide and urea increases and the intramolecular peptide–peptide hydrogen bonds decreases slightly with time. We show that the intramolecular peptide–peptide hydrogen bonds decreases and the total number of hydrogen bonds between the peptide and urea increases rapidly with time. The intramolecular hydrogen bonds that the peptide backbone formed in TFE/water and 2*M* urea had longer lifetimes than water and 8*M* urea. The intramolecular hydrogen bonds had the shortest lifetimes in water simulations (Table II).

Interaction of Peptide with Solvents

At the beginning of all simulations, the backbone amide hydrogens involved in α-helical hydrogen bonds were accessible to solvents. Once the simulations proceeded and the α-helical hydrogen bonds were disrupted, solvent penetration was observed. In general, the backbone am-

TABLE I. Occurrence (%) of Specific Intramolecular Hydrogen Bonds

	TFE	2*M* Urea	Water	4*M* Urea	8*M* Urea
MAG					
Phe^{5}(HN)-Gly^{1}(O)	–	38	–	–	–
Leu^{6}(HN)-Ile^{2}(O)	66	94	72	93	30
His^{7}(HN)-Gly^{3}(O)	82	6	6	5	0
Ser^{8}(HN)-Lys^{4}(O)	98	8	1	6	1
Ala^{9}(HN)-Lys^{4}(O)	–		1	–	
Ala^{9}(HN)-Phe^{5}(O)	99	98	9	97	94
Lys^{10}(HN)-Phe^{5}(O)	–	–	50	–	–
Lys^{10}(HN)-Leu^{6}(O)	100	100	46	100	65
Lys^{11}(HN)-Leu^{6}(O)	–	–	57	–	–
Lys^{11}(HN)-His^{7}(O)	94	99	42	95	38
Phe^{12}(HN)-His^{7}(O)	–	–	56	–	–
Phe^{12}(HN)-Ser^{8}(O)	99	98	32	97	29
Gly^{13}(HN)-Ser^{8}(O)	–	–	53	–	–
Gly^{13}(HN)-Ala^{9}(O)	100	98	23	91	–
Lys^{14}(HN)-Ala^{9}(O)	–	–	57	–	–
Lys^{14}(HN)-Lys^{10}(O)	99	97	25	76	–
Ala^{15}(HN)-Lys^{10}(O)	–	–	67	–	–
Ala^{15}(HN)-Lys^{11}(O)	95	94	25	67	–
Phe^{16}(HN)-Lys^{11}(O)	–	–	74	–	–
Phe^{16}(HN)- Phe^{12}(O)	93	92	24	57	–
Phe^{16}(HN)- Lys^{13}(O)	–	–	–	22	25
Val^{17}(HN)-Phe^{12}(O)	–	–	53	–	–
Val^{17}(HN)-Gly^{13}(O)	59	97	35	30	78
Gly^{18}(HN)-Gly^{13}(O)	23	–	46	–	–
Gly^{18}(HN)-Lys^{14}(O)	33	38	–	23	30
Gly^{18}(HN)-Met^{21}(O)	–	53	–	–	61
Gly^{18}(HN)-Asn^{22}(OD1)	–	–	–	30	–
Glu^{19}(HN)-Lys^{14}(O)	66	46	55	–	51
Glu^{19}(HN)-Ala^{15}(O)	–	34	–	–	21
Glu^{19}(HN)-Glu^{19}(OE2)	–	–	–	25	–
Ile^{20}(HN)-Ala^{15}(O)	82	46	70	23	67
Ile^{20}(HN)-Phe^{16}(O)	–	39	–	–	33
Met^{21}(HN)-Phe^{16}(O)	–	40	60	24	72
Met^{21}(HN)-Val^{17}(O)	34	28	–	–	–
Met^{21}(HN)-Gly^{18}(O)	32	–	–	–	–
Asn^{22}(HN)-Gly^{18}(O)	56	–	34	85	23
Asn^{22}(HN)-Glu^{19}(O)	36	–	–	–	–

The TPE, 2*M* urea, water, 4*M* urea, and 8*M* urea are measured at 300 K.

ide hydrogens closest to both ends of the initial α-helices were more prone to bind solvent. On the contrary, in all simulations, most of the carbonyl oxygens were accessible to solvent and most of the time had solvents molecules attached to them.

In Figure 8, the LTC and LUC per residue in each of the systems are reported. The LTC and LUC were calculated by determining the relative numbers of TFE, urea, and water molecules within a 0.6 nm shell surrounding each residue. In MAG-TFE/water, the concentration of TFE in close proximity to the helix is on average two times higher than the bulk. This indicates a strong tendency of the TFE molecules to coat the peptide. The residues are almost uniformly solvated by TFE, and little to no correlation exists between the LTC and either the nature of the residue or the secondary structure. In TFE, the interaction between the cosolvent and the peptide is weak.[21] Although a layer is formed over the surface of the peptide, the interactions between the peptide and TFE do not displace the peptide–peptide interactions. At the same time, TFE, despite having a lower dielectric constant than water, does not significantly disrupt hydrophobic interactions, which are important in the stability of peptide. In this respect, the action of TFE differs considerably from the action of urea. Not all aspects of the effect of TFE on the behavior of peptides in solution can be inferred from the simulations. For example, TFE is known to stabilize helix formation preferentially.

The LUC calculated over the full trajectory has an average value of 35, 45, and 57% (v/v) for the 2, 4, and 8*M* urea simulations. In case of 2*M* urea from the error bars, it appears that the LUC has small variations along the trajectory in hydrophilic residues, while in hydrophobic residues, variations are large. By increasing of concentration of urea, the variations of hydrophobic residues will decrease. Our comparative MD simulations reveal a correlation between the presence of α-helical structure and the decrease of LUC around the peptide. When urea was

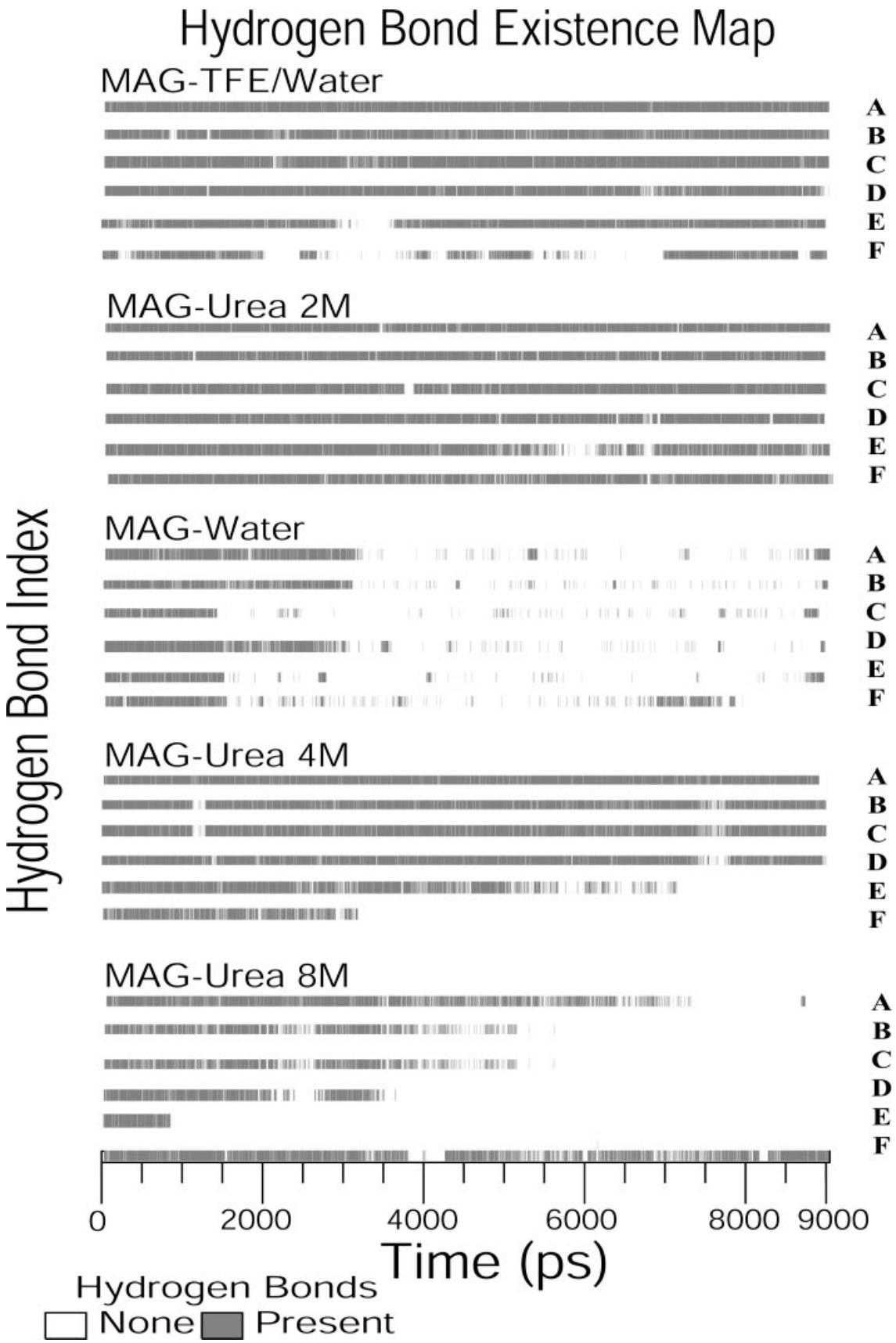

Fig. 6. Hydrogen bond existence map for six bonds in simulations: (**a**) Lys^{10}-Leu^{6}, (**b**) Lys^{11}-His^{7}, (**c**) Lys^{14}-Lys^{10}, (**d**) Phe^{12}-Ser^{8}, (**e**) Phe^{16}-Phe^{12}, and (**f**) Val^{17}-Gly^{13}.

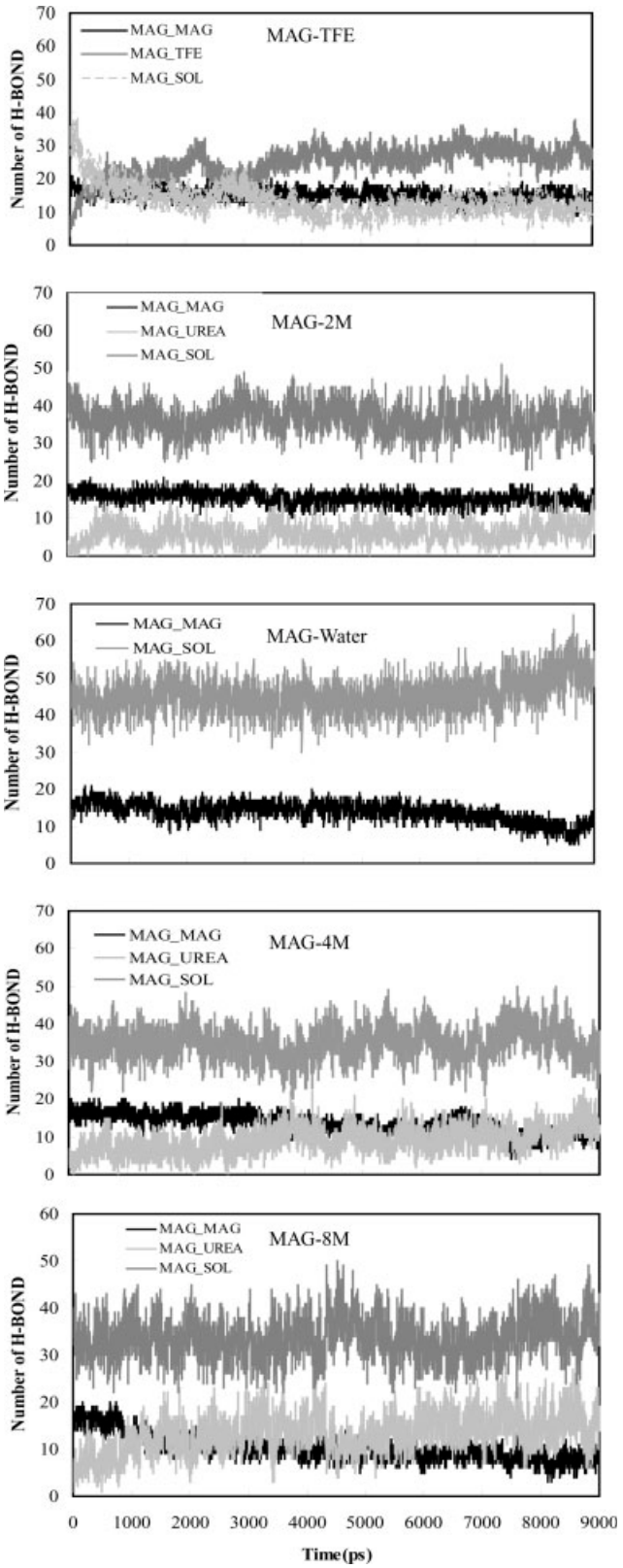

Fig. 7. The total number of hydrogen bonds between the peptide–peptide, peptide–TFE, peptide–water, and peptide–urea pairs.

applied as cosolvent, most of the first shell water molecules made hydrogen bonds with some of the peptide oxygens. The enhanced ability of water molecules to form hydrogen bonds with the peptide in the high concentration of urea (8*M*) simulations was also obvious when the water molecules accepted hydrogen bonds from the peptide. Indeed, when a water molecule in an 8*M* urea simulations became close to the peptide, it always accepted at least one hydrogen bond from it. Many of the early explanations of urea-dependent denaturation relied on chaotropic arguments: urea disorders water structure so that hydrophobic molecules are more easily solvated.[26] The urea molecules are believed to interact strongly with the protein and absorb onto hydrophilic residues situated at the surface of the protein.[8] The urea displaces interactions between the surface residues, leading to the swelling of the protein, the exposure of hydrophobic residues, and eventually to the penetration of water and denaturant into the core of the protein.

CONCLUSIONS

In this work, we reported MD simulations of magainin in water, TFE/water, and aqueous 2, 4, and 8*M* urea solutions and tried to analyze the structural properties under these conditions. The simulations show that in TFE/water the TFE molecules accumulate around magainin, which forms a matrix that partly excludes water molecules. By displacing water molecules from the surface of peptide, TFE has two effects: first, TFE molecules remove alternative hydrogen bonding partners and second, it creates a low dielectric environment.[21] These factors favor the formation of intramolecular hydrogen bonds.

At 8*M* urea, there are more direct interactions between the urea and solute, and the helix is destabilized. Urea interacts strongly with the peptide and absorb onto charged/hydrophilic residues situated at the surface of the protein. The urea displaces interactions between the surface residues, leading to the swelling of the peptide, the exposure of hydrophobic residues, and eventually to the penetration of water and denaturant into the core of the peptide. Our simulations, which concern the behavior of water and urea near the peptide, suggest that, at 8*M* urea, urea acts indirectly in the denaturation process. It decreases water mobility around the peptide and increases the ability to form peptide–water hydrogen bonds with longer lifetimes. By giving urea, molecules access to the polar groups of the peptide, thus it provides a better peptide solvation than pure water. Based on these results, urea catalyzed denaturation occurred by a combination of direct and indirect mechanism. Simulations of magainin in urea aqueous solution indicate that 2*M* urea appears to better solubilize hydrophobic solutes by, in effect, perturbing water and thereby preloading the solvent to accept nonpolar groups by subtle disruption of water's preferred structure and reorientation of the waters around its polar atoms.[26] At 2*M* urea, the interaction of urea molecules and nonpolar residues are weak, therefore, the presence of urea molecules decreases the interactions of water mole-

TABLE II. Peptide Backbone–Backbone Hydrogen Bond Mean Lifetime (ps)

	TFE	2*M* urea	Water	4*M* urea	2*M* urea
MAG					
Lys^{10}(HN)-Leu^{6}(O)	47.17	33.04	11.18	37.94	10.37
Lys^{11}(HN)-His^{7}(O)	21.09	31.02	9.47	21.47	7.50
Phe^{12}(HN)-Ser^{8}(O)	33.61	36.23	27	30.73	15.11
Gly^{13}(HN)-Ala^{9}(O)	29.55	29.46	12.05	22.43	17.53
Lys^{14}(HN)-Lys^{10}(O)	35.52	33.83	8.68	21.74	37.42
Ala^{15}(HN)-Lys^{11}(O)	24.37	23.53	12.05	12.41	24.50
Phe^{16}(HN)-Phe^{12}(O)	26.16	17.10	11.20	10.97	28.85
Val^{17}(HN)-Gly^{13}(O)	12.38	18.65	8.22	10.25	11.19

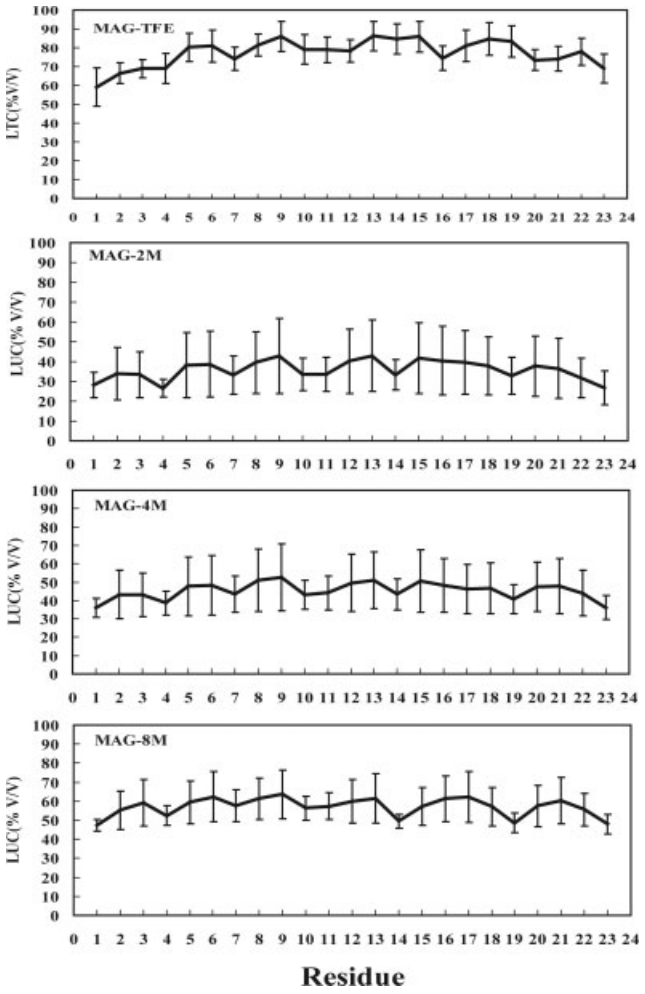

Fig. 8. Average local TFE concentration and local urea concentration within a distance of 0.6 nm from the C-α atom of each residue of magainin, calculated using the full trajectory of all simulations. Bars indicate the standard deviations.

cules with hydrophilic groups. With pervious studies,[26] at low concentration of urea, urea disorder water structure so that hydrophobic molecules are more easily solvated. It is obvious that at 2*M* urea, urea could not deteriorate the peptide secondary structure during the simulation time from an initial helix structure and also the peptide remained stable in our time scale.

ACKNOWLEDGMENTS

We thank Erfani Moghaddam for a critical reading of the manuscript. The support of the Tarbiat Modarres University is gratefully acknowledged. The invaluable beneficiary of Tarbiat Modarres University Molecular Modeling Center is also gratefully acknowledged.

REFERENCES

1. Velicelebi G, Sturtevant JM. Thermodynamics of the denaturation of lysozyme in alcohol–water mixtures. Biochemistry 1979; 18:1180–1186.
2. Fu L, Freire E. On the origin of the enthalpy and entropy convergence temperatures in protein folding. Proc Natl Acad Sci USA 1992;89:9335–9338.
3. Buck M. Trifluoroethanol and colleagues: co-solvents come of age. Recent studies with peptides and proteins. Q Rev Biophys 1998; 31:297–355.
4. Cacace MG, Landau EM, Ramsden JJ. The Hofmeister series: salt and solvent effects on interfacial phenomena. Q Rev Biophys 1997;30:241–277.
5. Robinson GW, Cho CH. Role of hydration water in protein unfolding. Biophys J 1999;77:3311–3318.
6. Pace CN. Determination and analysis of urea and guanidine hydrochloride denaturation curves. Methods Enzymol 1986;134: 266–280.
7. Nozaki Y, Tanford C. The solubility of amino acids and related compounds in aqueous solutions. J Biol Chem 1963;238:4074–4081.
8. Wallqvist A, Covell DG, Thirumalai D. Hydrophobic interactions in aqueous urea solutions with implications for the mechanism of protein denaturation. J Am Chem Soc 1998;120:427–428.
9. Trzesniak D, van der Vegt NFA, van Gunsteren WF. Computer simulation studies on the solvation of aliphatic hydrocarbons in 6.9 M aqueous urea solution. Phys Chem Chem Phys 2004;6: 697–702.
10. Smith LJ, Dobson CM, van Gunsteren WF. Side-chain conformational disorder in a molten globule: molecular dynamics simulations of the A-state of human α-lactalbumin. J Mol Biol 1999;286: 1567–1580.
11. Kamoun PP. Denaturation of globular-proteins by urea-breakdown of hydrogen or hydrophobic bonds. Trends Biochem Sci 1998;13: 424–425.
12. Smith LJ, Berendsen HJC, van Gunsteren WF. Computer simulations of urea-water mixtures: a test of force field parameters for use in biomolecular simulations. J Phys Chem A 2004;108: 1065–1071.
13. Tobi D, Elber R, Thirumalai D. The dominant interaction between peptide and urea is electrostatic in nature: a molecular dynamics simulation study. Biopolymers 2003;68:359–369.
14. Bennion BJ, Daggett V. The molecular basis for the chemical denaturation of proteins by urea. Proc Natl Acad Sci USA 2003; 100:5142–5147.
15. Zou Q, Habermann-Rottinghaus SM, Murphy KP. Urea effects on protein stability: hydrogen bonding and the hydrophobic effect. Proteins 1998;31:107–115.

16. Hong DP, Hoshino M, Kuboi R, Goto Y. Clustering of fluorine-substituted alcohols as a factor responsible for their marked effects on proteins and peptides. J Am Chem Soc 1999;121:8427–8433.
17. Jasanoff A, Fersht AR. Quantitative determination of helical propensities from trifluoroethanol titration curves. Biochemistry 1994;33:2129–2135.
18. Luo P, Baldwin RL. Mechanism of helix induction by trifluoroethanol: a framework for extrapolating the helix-forming properties of peptides from trifluoroethanol/water mixtures back to water. Biochemistry 1997;36:8413–8421.
19. Diaz MD, Fioroni M, Burger K, Berger S. Evidence of complete hydrophobic coating of bombesin by trifluoroethanol in aqueous solution: an NMR spectroscopic and molecular dynamics study. Chem—Eur J 2002;8:1663–1669.
20. Fioroni M, Burger K, Mark AE, Roccatano D. A new 2,2,2-trifluroethanol model for molecular dynamics simulations. J Phys Chem B 2002;104:12347–12354.
21. Roccatano D, Colombo G, Fioroni M, Mark AE. Mechanism by which 2,2,2-trifluoroethanolywater mixtures stabilize secondary-structure formation in peptides: a molecular dynamics study. Proc Natl Acad Sci USA 2002;99:12179–12184.
22. Gesell J, Zasloff M, Opella SJ. 1997. Two-dimensional ^{1}H NMR experiments show that the 23-residue magainin antibiotic peptide is an α-helix in dodecylphosphocholine micelles, sodium dodecylsulfate micelles, and trifluoroethanol/water solution. J Biomol NMR 1997;9:127–135.
23. Grant E, Jr, Beeler TJ, Taylor KM, Gable K, Roseman MA. Mechanism of magainin 2a induced permeabilization of phospholipids vesicles. Biochemistry 1992;31:9912–9918.
24. Sheynis T, Sykora J, Benda A, Kolusheva S, Hof M, Jelinek R. Bilayer localization of membrane-active peptides studied in biomimetic vesicles by visible and fluorescence spectroscopies. Eur J Biochem 2003;270:4478–4487.
25. Kandasamy SK, Larson RG. Binding and insertion of α-helical anti-microbial peptides in POPC bilayers studied by molecular dynamics simulations. Chem Phys Lipids 2004;132:113–132.
26. Lindahl E, Hess B, van der Spoel D. GROMACS 3.0: a package for molecular simulation and trajectory analysis. J Mol Model 2001;7:306–317.
27. Van Der Spoel D, Lindahl E, Hess B, Groenhof G, Mark AE, Berendsen HJ. GROMACS: fast, flexible, and free. J Comput Chem 2005;26:1701–1718.
28. Berendsen HJC, Postma JPM, van Gunsteren WF, Di Nola A, Haak JR. Molecular dynamics with coupling to an external bath. J Chem Phys 1984;81:3684–3690.
29. Van Gunsteren WF, Billeter SR, Eising AA, Hünenberger PH, Krüger P, Mark AE, Scott WRP, Tironi IG. Biomolecular simulations: the GROMOS96 manual and user guide. 1996. Zürich VdF Hochschulverlag ETHZ.
30. Hess B, Bekker H, Berendsen HJC, Fraaije JGEM. LINCS: a linear constraint solver for molecular simulations. J Comput Chem 1997;18:1463–1472.
31. Darden T, York D, Pedersen L. Particle Mesh Ewald: an N log (N) method for Ewald sums in large systems. J Chem Phys 1993; 98:1463–1472.
32. Berendsen JC, van der Spoel D, van Drunen R. GROMACS: a message-passing parallel molecular dynamics implementation. Comput Phys Commun 1995;91:43–56.
33. Berendsen HJC, Grigera JR, Straatsma TP. The missing term in effective pair potentials. J Phys Chem 1987;91:6269–6271.
34. Marcus Y.Wiley series in solution chemistry, Vol. 4: The properties of solvents. Chichester, NY: Wiley; 1998.
35. Kabsch W, Sander C. Dictionary of protein secondary structure: pattern-recognition of hydrogen-bonded and geometrical feature. Biopolymers 1993;33:2577–2637.
36. Zou Q, Bennion BJ, Daggett V, Murphy K. The molecular mechanism of stabilization of proteins by TMAO and its ability to counteract the effects of urea. J Am Chem Soc 2002;124:1192–1202.